Materials and Structures / Matériaux et Constructions, Vol. **36**, August-September 2003, pp 426-438

Chemomechanics of concrete at finer scales

F.-J. Ulm
Department of Civil and Environmental Engineering, Massachusetts Institute of Technology, Cambridge, MA 02139, USA

ABSTRACT

Concrete, like many other materials (whether man-made, geological or biological), is a highly heterogeneous material with heterogeneities that manifest themselves at multiple scales. As new experimental techniques such as nanoindentation have provided unprecedented access to micro-mechanical properties of materials, it becomes possible to identify the mechanical effects of chemical reactions at the micro-scale, where the reactions occur, and trace these micro-chemo-mechanical effects through upscaling techniques to the macro-scale. The focus of this paper is to review recent developments of a micro-chemomechanics theory which ultimately shall make it possible to capture chemomechanical deterioration processes at the scale where physical chemistry meets mechanics. This is illustrated through application of the theory to early-age concrete and calcium leaching, and an outlook to biologically mediated deterioration processes in solid materials is given.

RÉSUMÉ

Le béton comme beaucoup d'autres matériaux, soit artificiels, géologiques ou biologiques, est un matériau très hétérogène, dont les hétérogénéités se manifestent à de multiples échelles. Comme des techniques expérimentales nouvelles, telle la nano-indentation, ont donné un accès non-précédent aux propriétés micromécaniques des matériaux, il est possible d'identifier les effets mécaniques des réactions chimiques à l'échelle microscopique, où les réactions ont lieu, et tracer ces effets au travers des méthodes de changement d'échelle vers l'échelle macroscopique. Cet article fait le point sur le développement d'une modélisation micro-chimico-mécanique qui a comme but de modéliser la détérioration chimico-mécanique à partir de l'échelle physico-chimique. Ces développements sont illustrés au travers des applications au béton au jeune âge et à la lixiviation des bétons. Enfin, l'extension de cette modélisation aux processus de détérioration bio-chimique des matériaux est mise en perspective.

DEDICATION

This review paper on chemomechanics which is based on the Robert L'Hermite award lecture I gave during the RILEM week in Madrid in September 2002, presents collective research results of my research group at M.I.T., obtained in 1999-2002. I am deeply indebted to my students and associates who made this research and the excitement happen: To Georgios Constantinides (SM 2002), to whom I owe the multiscale representation of concrete, and the research into nanoindentation; To Dr. Franz H. Heukamp (DSc 2002), to whom I owe the investigation of the triaxial strength and deformation behavior of calcium leached cementitious materials; To Emilio C. Silva, who solved the question how to integrate biological activity in the chemomechanics theory; and many more. To my postdoctoral research associates: Dr. Marc Mainguy, now with IFP France, to whom I owe the investigation of the (negligible) effects of cracks on concrete deterioration processes, Dr. Eric Lemarchand, now Chargé de Recherche of CNRS in Lille (LML UMR 8107, Villeneuve d'Ascq, France), who taught us at M.I.T. how to use continuum micromechanics for stiffness and strength properties of concrete and bones; Dr. Christian Hellmich, now back at his home institute, the Technical University of Vienna (Institute of

Editorial note
Prof. Franz-Josef Ulm presented a lecture of this paper at the 2002 RILEM Annual Meeting in Madrid, Spain, when he was awarded the 2002 Robert L'Hermite Medal in recognition of his work in the field of durability mechanics.
He is a RILEM Senior Member and Associate Editor for Concrete Science and Engineering.

strength of materials, Austria), who in his PhD-thesis developed the basis of the macroscopic thermochemo-mechanics theory into a versatile engineering mechanics theory that is now employed in innovative shotcrete tunneling applications, and to whom I owe my current understanding that continuum mechanics applies at very fine scales of concrete and bone, right above the molecular level; Dr. Olivier Bernard, now with Oxand SA, Montigny-sur-Loing, France, who developed with us the multiscale micromechanics theory for aging elasticity of cement-based materials. To Dr. John T. Germaine, my colleague and friend at M.I.T., whose unequaled rigor in experimental research on engineering materials guides the experimental research of my group. The results presented in this paper would not have been achieved without the exciting collaboration and friendship with the most gifted mechanics researchers and educators: Prof. Olivier Coussy (Institut Navier, France), my teacher, friend and mentor in mechanics, who instilled in me the beauty of (poro)mechanics; Prof. Luc Dormieux (ENPC-LMSGC, France), to whom I owe the investigation of micro-poromechanics; and Dr. Paul Acker (Lafarge, France), who is at the origin of my choice of and approach to concrete research at the interface of materials science and structural mechanics.

I dedicate this paper to the pioneers of what is now known as 'durability mechanics of concrete': To Professor Zdeněk P. Bažant, Northwestern University, Evanston, Illinois, on the occasion of his 65th birthday. To Professor Folker H. Wittmann on the occasion of his retirement from ETH Zurich, Switzerland. Their eminent contributions, leadership, vision, passion and friendship have profoundly marked, inspired and challenged me, as so many others of my generation of concrete mechanicians and engineers.

1. INTRODUCTION

One of the keys to the modeling of chemomechanical couplings in materials is the choice of an appropriate thermodynamic system for the description of the governing conservation laws, including mass, energy and entropy conservation. We owe this insight to the works of Coussy [1], who provided the macroscopic framework for modelling chemomechanical couplings in porous materials as an extension and refinement of Biot's saturated porous media theory. The thermodynamic system in the Biot-Coussy theory of poromechanics, is the *open* macroscopic porous material, considered as a superposition in time and space of a solid phase and n fluid phases that exchange matter through its boundary with the outside. Chemomechanics in this theory is associated with phase change phenomena in between the fluid phases or in between the fluid phases and the solid phase [2], inducing time dependent deformation, both reversible (chemoelasticity) and irreversible (chemoplasticity). This leads, in this macroscopic theory, to an advanced internal variable theory, in which a reaction extent or a reaction degree is added to the set of standard solid mechanics state variables (strain, temperature, plastic strain, damage, etc.; see *e.g.* [3]). The theory has been employed in many engineering applications to capture coupled chemomechanical phenomena in concrete mechanics: thermo-chemo-mechanical couplings in early-age concrete [4-7] and shotcrete [8]; early-age concrete strength growth as chemoplastic hardening [9, 10]; hydration heat as thermochemical coupling [11, 12]; chemoplastic softening in rapidly heated concrete [13]; chemoelasticity of ASR-expansion [14-17]; chemoplasticity of ASR-expansion [18], chemoporoplasticity of calcium leaching [13], and so on. The strength of the macroscopic theory is that it makes it possible to lump a large number of complex chemical reactions into one or several macroscopic state variables, the evolution of which can be determined with almost standard macroscopic material tests. On the other hand, this macroscopic approach has one fundamental drawback which is intrinsically related to the choice of the macroscopic system; that is, the choice of chemomechanical state variables is not unique, in contrast to the chemophysical phenomena at stake which are certainly unique for any specific (*i.e.* identified) chemomechanical deterioration process. The dilemma is due to the fact that the chemical processes at stake typically occur at much smaller scales than the macroscopic scale, where chemical reactions express themselves through loss of stiffness, strength, frictional capacity, cohesion, deleterious expansion, and so on. This recognized limit of the macroscopic theory has prompted research into the development of a micro-chemomechanics theory. The premise of such a theory is to capture chemomechanical deterioration processes at *the* scale where physical chemistry meets mechanics. The same holds true for coupled biomechanical processes in solid materials, in which microorganisms deteriorate solid materials leading to premature failure of materials and structures (biocorrosion in sewer pipes; increased risk of bone fracture due to osteoporosis, etc.).

The aim of this review paper is two fold: (1) to review recent developments in micro-chemomechanics theory, and (2) to identify relevant macroscopic state variables from the scale where physical chemistry (or biochemistry) meets mechanics. This will be illustrated through several application of this theory to early-age concrete, concrete deterioration by calcium leaching, and finally to biologically mediated deterioration processes.

2. MICRO-CHEMOMECHANICS

Physical chemistry focuses on the chemical agents in an undeformable system. By contrast, chemomechanics at the microscale focuses on the deformable solid in the porous material subjected to a chemical attack on the solid-fluid interface. This comes to choose the solid matter, at the microscale, as the thermodynamic system, which as we will see below provides the missing link between physical chemistry (or biochemistry) and mechanics. This solid matter is subjected at a part of its boundary, say $\Gamma \subseteq \partial V_s$, to a chemical reaction which adds (precipitation) or removes (dissolution) matter.

2.1 Chemical porosity

The total mass of the solid enclosed in an r.e.v. $|V|$ is:

$$|V| m_s = \int_{V_s} \rho_s dV \tag{1}$$

and its variation reads:

$$\frac{dm_s}{dt}=\frac{1}{|V|}\int_{V_s}\left(\frac{d\rho_s}{dt}+\rho_s\mathrm{div}(\underline{u}^s)\right)dV+$$
$$\frac{1}{|V|}\int_{\partial V_s}[[\rho_s\underline{u}^s]]\cdot\underline{n}_s da \qquad (2)$$

The first term expresses the mass conservation in the solid bulk, that is at the microlevel of the solid phase; while the second term refers to the mass rate jump that is induced by precipitation ($[[\rho_s\underline{u}^s]]\cdot\underline{n}_s\geq 0$) or dissolution ($[[\rho_s\underline{u}^s]]\cdot\underline{n}_s\leq 0$) that occurs at the boundary Γ of the solid phase:

$$[[\rho_s\underline{u}^s]]\cdot\underline{n}_s=\eta\rho_c\underline{u}^c\cdot\underline{n}_s \qquad (3)$$

where $\eta=1$ on Γ, and $\eta=0$ on $\partial V_s-\Gamma$; ρ_c is the mass density of the chemical species, and $\underline{u}^c\cdot\underline{n}_s d\Gamma\times dt$ the associated infinitesimal volume of the surface layer that is chemically added to or chemically removed from the solid phase. It is readily understood that this surface layer gives rise to a change in macroscopic porosity. More precisely, if we introduce the Lagrangian porosity:

$$\phi=\frac{V_f}{|V|}=\frac{V_t-V_s}{|V|}\approx(1+E_v)-\frac{V_s}{|V|} \qquad (4)$$

where V_t, V_f and V_s are the volumes of the porous material, the fluid phase and the solid phase in the current (deformed) configuration, the total change of the Lagrangian porosity is:

$$\frac{d\phi}{dt}=\frac{dE_v}{dt}-\frac{V_s}{|V|}\left\langle\frac{d\varepsilon_v^s}{dt}\right\rangle_{V_s}-\frac{1}{|V|}\int_{\partial V_s}[[\underline{u}^s]]\cdot\underline{n}_s da \qquad (5)$$

The first two terms in this relation represent the change in porosity due to mechanical loading, where $\left\langle\frac{d\varepsilon_v^s}{dt}\right\rangle_{V_s}=\frac{1}{V_s}\int_{V_s}\mathrm{div}(\underline{u}^s)dV$ is the volume average of the rate of relative volume change in the solid phase. In turn, the third term represents the chemically induced porosity change:

$$\frac{d\phi^c}{dt}=-\frac{1}{|V_s|}\int_{\partial V_s}\eta\underline{u}^c\cdot\underline{n}_s da=-\frac{1}{|V|}\int_{\Gamma}\underline{u}^c\cdot\underline{n}_s d\Gamma \qquad (6)$$

The chemical porosity ϕ^c appears as an appropriate state variable to describe volume changes related to the chemical reaction that occur at the boundary Γ of the solid phase.

2.2 Driving forces of chemomechanics

We want to determine the driving forces of the chemomechanical processes in the porous material. Since we are interested in the solid's response, the thermodynamic system we consider is the solid phase (volume V_s). To simplify the presentation, we will assume isothermal and quasi-static evolutions. The energy transformations are expressed by the Clausius-Duhem inequality, which states that the external energy supply to the solid, $d\mathcal{W}_{ext}^s$, which is not stored as free energy dW^s in the solid system, is dissipated into heat form:

$$\frac{d\mathcal{D}}{dt}=\frac{d\mathcal{W}_{ext}^s}{dt}-\frac{dW^s}{dt}\geq 0 \qquad (7)$$

For the chemomechanical solid system under consideration, the external energy supply has two origins:

The first is of mechanical origin due to volume forces in the solid (term of the form $\rho_s\underline{f}dV$), and surface tension $\underline{t}_s=\underline{\underline{\sigma}}\cdot\underline{n}_s$, where $\underline{\underline{\sigma}}$ is the stress tensor in the solid phase. These forces supply a work rate along the velocity field $\underline{u}^s$. Thus, by application of the theorem of virtual work rate,

$$\frac{dW_{ext}^m}{dt}=\int_{V_s}\underline{u}^s\cdot\rho_s\underline{f}dV+\int_{\partial V_s}\underline{u}^s\cdot\underline{t}_s da=$$
$$\int_{V_s}\underline{\underline{\sigma}}:\frac{d\underline{\underline{\varepsilon}}^s}{dt}dV-p\int_{\partial V_s}[[\underline{u}^s]]\cdot\underline{n}_s da \qquad (8)$$

where we made use of $2d\underline{\underline{\varepsilon}}^s/dt=\mathrm{grad}\underline{u}^s+{}^t\,\mathrm{grad}\underline{u}^s$, the symmetry of the stress tensor $\underline{\underline{\sigma}}$, the local equilibrium in the solid phase, $\mathrm{div}\underline{\underline{\sigma}}+\rho_s\underline{f}=0$, and the stress continuity at the solid-fluid interface ∂V_s, *i.e.* $\underline{\underline{\sigma}}\cdot\underline{n}_s=-p\underline{n}_s$, where p is the fluid pressure assumed constant in the pore space. Applied to the r.e.v. with regular stress or strain boundary conditions, it can be shown with the help of the Hill-Mandel lemma (see for instance [20]) that the external mechanical work rate (Equation (8)) can be developed in the form:

$$\frac{dW_{ext}^m}{dt}=|V|\left[\underline{\underline{\Sigma}}:\frac{d\underline{\underline{E}}}{dt}+p\frac{d\phi}{dt}\right] \qquad (9)$$

where $\underline{\underline{\Sigma}}=\langle\underline{\underline{\sigma}}\rangle_V$ = macroscopic stress tensor; and $d\underline{\underline{E}}/dt=\langle d\underline{\underline{\varepsilon}}/dt\rangle_V$ = macroscopic strain rate.

The second external energy supply to the solid results from the action of the chemical potential of the solute, μ^{sol}, at the boundary Γ, which provides energy to the solid along a molar flux $J_N=\left(\frac{\rho_c}{\mathcal{M}}\right)\underline{u}^c\cdot\underline{n}_s=-\left(\frac{\rho_c}{\mathcal{M}}\right)\underline{u}^c\cdot\underline{n}_f$ (with $(\rho_c/\mathcal{M})$ = number of moles per unit solid volume of the chemical species precipitating or dissolving from the solid):

$$\frac{dW_{ext}^c}{dt}=\int_{\Gamma}\mu^{sol}\left(\frac{\rho_c}{\mathcal{M}}\right)\underline{u}^c\cdot\underline{n}_s d\Gamma=-\mu^{sol}\left(\frac{\rho_c}{\mathcal{M}}\right)\frac{d\phi^c}{dt}|V| \qquad (10)$$

where we assumed μ^{sol} constant along Γ.

Finally, we need to express the change in free energy of the solid, which involves at least two components: the elasticity potential ψ_s^{el} (of dimension $[\psi_s^{el}]$ =$L^{-1}MT^{-2}$), and the chemical potential μ_c (of dimension $[\mu_c] = L^2MT^{-2} \times MOL^{-1}$) of the chemical species in the solid phase:

$$W_s = \int_{V_s} \psi_s dV = \int_{V_s} \left(\psi_s^{el} + \left(\frac{\rho_c}{\mathcal{M}} \right) \mu_c \right) dV \tag{11}$$

The elasticity potential ψ_s^{el} represents the recoverable (elastic) energy volume density stored by externally applied work into the solid phase; the chemical potential μ_c expresses the energy stored as chemical bonds in the solid phase. The total time derivative of Equation (11) reads:

$$\frac{dW^s}{dt} = \int_{V_s} \left[\frac{d\psi_s}{dt} + \psi_s \frac{d\varepsilon_v^s}{dt} \right] dV + \int_\Gamma \left(\psi_s^{el} + \left(\frac{\rho_c}{\mathcal{M}} \right) \mu_c \right) \underline{u}^c \cdot \underline{n}_s d\Gamma \tag{12}$$

Last, collecting the different components from Equations (9), (10) and (12), the dissipation of chemomechanical energy supplied to the solid is shown to be the sum of two terms [21]:

$$\frac{d\mathcal{D}}{dt} = |V| \left(\varphi_1^s + \varphi^c \right) \geq 0 \tag{13}$$

- The first term φ_1^s represents the dissipation rate associated with mechanical deformation of the solid phase. It is similar to the one of the intrinsic solid dissipation emerging from the Biot-Coussy theory of macroscopic poromechanics [1], if we replace the total porosity ϕ in the theory by the mechanical porosity $\phi^m = \phi - \phi^c$

$$\varphi_1^s = \underline{\underline{\Sigma}} : \frac{d\underline{\underline{E}}}{dt} + p \left(\frac{d\phi}{dt} - \frac{d\phi^c}{dt} \right) - \frac{d\Psi_s}{dt} \geq 0 \tag{14}$$

with:

$$\frac{d\Psi_s}{dt} = \frac{1}{|V|} \int_{V_s} \left(\frac{d\psi_s}{dt} + \psi_s \frac{d\varepsilon_v^s}{dt} \right) dV \tag{15}$$

The modeling of the deformation behavior of the porous material that occurs simultaneously with chemical reactions, can make use of the rich body of macroscopic models available in the porous media literature.

- The second term φ^c represents the dissipation related to the chemical reaction at the boundary of the solid phase, and the associated increase of the chemical porosity (defined by Equation (6)):

$$\varphi^c = -\mathcal{A} \circ \frac{d\phi^c}{dt} = \frac{1}{|V|} \int_\Gamma A \times J_N d\Gamma \geq 0 \tag{16}$$

with

$$A = \mu^{sol} - \mu_c - \left(\frac{\mathcal{M}}{\rho_c} \right) \left(\psi_s^{el} + p \right) \tag{17}$$

where A is the chemical affinity, *i.e.* the driving force of the molar flux $J_N = \left(\frac{\rho_c}{\mathcal{M}} \right) \underline{u}^c \cdot \underline{n}_s$. The quantity $\Delta G = \mu^{sol} - \mu_c$ is the Gibbs energy; that is the pure chemical driving force of the precipitation/dissolution process. In addition, due to the multiphase nature of the porous media and the deformability of the solid phase, two additional quantities affect the chemomechanical driving force: the local elastic energy ψ_s^{el}, and the fluid pressure p. Following standard thermodynamics, the identification of affinity $A = \Delta G - (\mathcal{M}/\rho_c)(\psi_s^{el} + p)$ as driving force implies that the local kinetic law of the precipitation or dissolution process is one which relates the molar flux J_N to the chemical affinity:

$$\text{on } \Gamma : J_N = J_N(A); A \times J_N(A) \geq 0 \tag{18}$$

Remarkably, since $J_N \propto \underline{u}^c \cdot \underline{n}_s < 0$ in a dissolution process, $A < 0$, so that the chemical dissipation remains locally greater or equal than zero. Hence, since $\psi_s^{el} \geq 0$ and $p \geq 0$, it follows that the elastic energy stored in the microstructure and a non-zero fluid pressure will actually increase the intensity of the dissolution process; and for a precipitation process it is the inverse. This effect of strain and pressure on the affinity must be checked, from case to case, relative to the pure chemical potential difference $\Delta G = \mu^{sol} - \mu_c$.

In summary, the brief study of the micro-to-macroscopic energy transformations for the solid as thermodynamic system, allows one to break down the chemomechanical behavior (at the macro-scale) of materials into two components: a purely poromechanics behavior (which is well established for engineering materials by the Biot-Coussy theory of poromechanics [1]), and a chemomechanical precipitation or dissolution process, which is witnessed by the solid as a moving boundary. This split of the macroscopic response allows one to capture many coupled chemomechanical phenomena in geomaterials and biomaterials; some of which are developed below.

3. APPLICATION TO CONCRETE

The application of the micro-chemomechanics theory requires a breakdown of the material into the scale where the material can be represented as a porous material. This is a particular difficult task for cementitious materials due to the high level of heterogeneity of the material that manifests itself at multiple scales. A rough breakdown of characteristic mechanical length scales of cementitious materials is displayed in Fig. 1 [22].

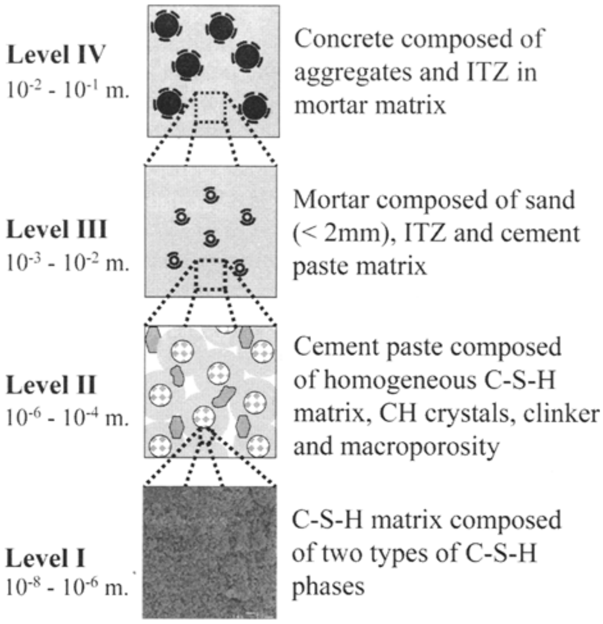

Fig. 1 - The four-level microstructure of concrete [22].

1. Level I: The lowest level we consider is the one of the C-S-H matrix that forms at early ages by the hydration of C_3S and C_2S[1].

This level of a characteristic length scale of 10^{-8}-10^{-6} m, is the smallest material length scale that is, at present, accessible by mechanical testing, *i.e.* nanoindentation. At this scale, it is now well established that the C-S-H exist in, at least, two different forms with different volume fractions [23, 24] and elastic properties [25, 26]. The morphology of the two types of C-S-H is correlated with two different processes of hydration of clinker compounds. During the early stages of hydration, nucleation and growth of C-S-H occurs at the surface of the cement grains, leading to the softer outer products. With the hydration progressing, the cement grains are covered by a growing layer of C-S-H and the hydration is controlled by the diffusion process through this layer.

While outer products are still formed, new C-S-H is primarily formed in a space confined by the existing C-S-H layer; and these new C-S-H have a higher density, leading to an on-average higher stiffness of the inner product C-S-H. This is displayed in Fig. 2 (Top) which displays the stiffness histogram of nanoindentation results of a hardened cement paste (w/c = 0.5). The reason for the difference in stiffness between inner and outer product is attributed to the difference in C-S-H gel porosity at a scale still below. However, this gel porosity (28% in average) is of a characteristic size of some water molecules (4-5 water molecules, *i.e.* a size on the order of 10^{-9} m), so that the water present at this scale cannot be considered as a bulk water phase [27, 28]. In turn, at the considered level I, the C-S-H matrix can be considered as a two-phase solid material, composed of a stiffer inclusion phase (C-S-H_b-phase), embedded into a softer matrix phase (C-S-H_a-phase). The governing variables at this scale are the volume fractions of the two phases, and the intrinsic material properties of the two phases.

[1] *The cement's chemistry abbreviation will be used in this paper (C_3S = 3 CaO SiO_2, C_2S = 2 CaO SiO_2, C_3A = 3 CaO Al_2O_3, C_4AF = 4 CaO Al_2O_3 Fe_2O_3).*

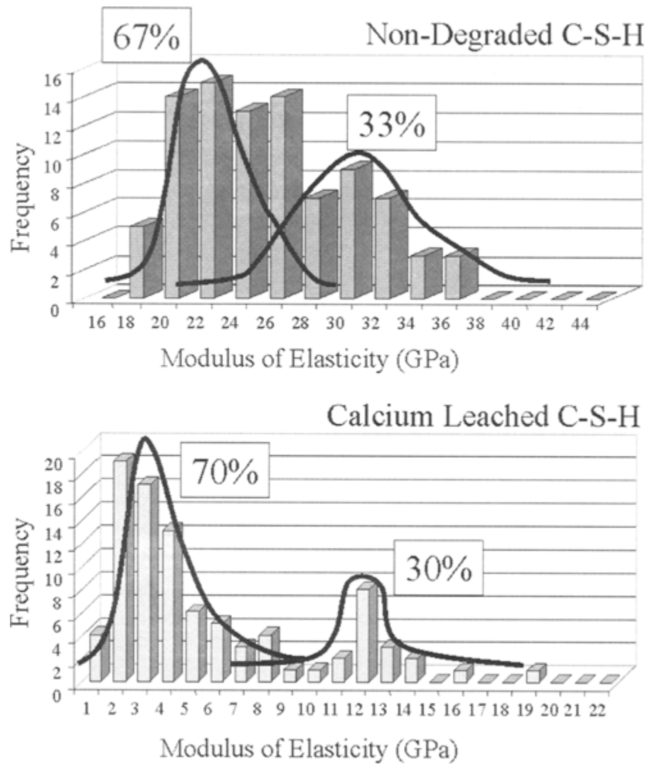

Fig. 2 - Histogram of elasticity moduli obtained by nanoindentation on Calcium-Silica-Hydrates (C-S-H); w/c = 0.5: Top: non-degraded C-S-H, Bottom: calcium leached C-S-H. The histogram allows the identification of the two types of C-S-H in cementitious materials that affect the macroscopic elasticity of concrete materials [26].

2. Level II: The C-S-H matrix together with unhydrated cement products (*i.e.* the four clinker phases X = C_3S, C_2S, C_3A, C_4AF), large Portlandite crystals (CH = $Ca(OH)_2$), aluminates and macro-porosity in the case of high water-to-cement ratio materials (roughly w/c>0.4) forms the cement paste, and is referred to as Level II (10^{-6}-10^{-4}m). It is the scale at which cementitious materials can be considered as porous materials. The intrinsic material properties of the elementary components are now well known from nanoindentation tests [29, 25, 26].
3. Level III (10^{-3}-10^{-2} m) refers to mortar; that is a three phase composite material composed of a cement paste matrix, sand particle inclusions, and an Interfacial Transition Zone (ITZ). The volume fractions of these three phases are fixed in time, that is they are not affected by chemical reactions.
4. Concrete as a composite material is considered on Level IV (10^{-2}-10^{-1}m). Similar to Level III, concrete at this scale is a three-phase material composed of aggregates (> 2 mm) embedded in a continuous homogeneous mortar matrix and an ITZ; and the required volume fractions are also fixed in time.

It is worth noting that the four levels described above respect the separability of scale condition; that is each scale is separated by the next one by at least one order of length magnitude. This makes it possible to apply linear and nonlinear continuum micromechanics to upscale material properties [38].

3.1 Early-age concrete

Starting point of modeling early-age concrete is level I, that is the scale of the C-S-H matrix. At this scale, the two types of C-S-H, which are the reaction products of the hydration of the two clinker phases C_3S and C_2S, result from two different hydration processes: The low-density C-S-H_a-phase corresponding to the outer products, is formed during the nucleation and growth process; the high-density C-S-H_b-phase corresponding to the inner products, is formed during the diffusion controlled hydration reaction. The kinetics of these processes has been focus of intensive research in cement chemistry, delivering reaction degrees for C_3S and C_2S hydration. The link between physical chemistry (hydration degrees) and mechanical properties is provided by the volume fractions of the two C-S-H-phases. Use of the volume fractions in appropriate homogenization schemes that capture the strong matrix-inclusion morphology of cementitious materials (*e.g.* Mori-Tanaka scheme [32]; see also [38]), delivers the composite stiffness of the C-S-H matrix (level I), cement paste (level II), mortar (level III) and concrete (level IV); see Fig. 3.

While the development of this four-level homogenization scheme, presented in [33], goes beyond the scope of this paper, it is worth noting that the intrinsic stiffness of all involved phases do not change, neither in time, nor from one cement-based material to another. The only parameters that change, at early ages, are the volume fractions, which depend primarily on the *w/c*- ratio.

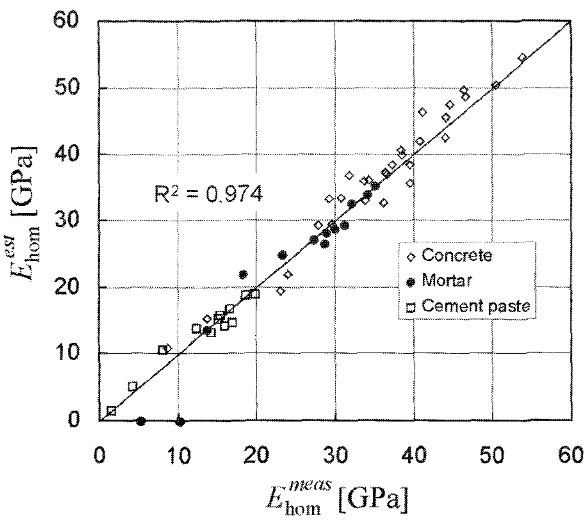

Fig. 3 - Predictive capability of a four-level homogenization model: predicted versus measured E-modulus [33].

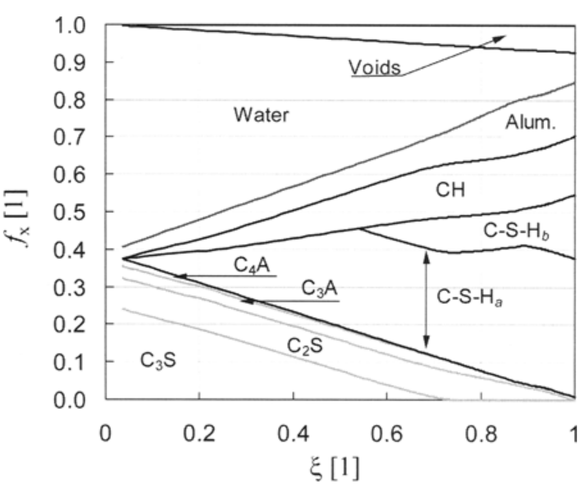

Fig. 4 – Evolution of volume fractions of the phases of a w/c=0.5 cement paste (Level II) as a function of the hydration degree [33].

In turn, we will address here the application of the micro-chemomechanics theory to level II, which is the level where the material can be considered as a porous material. The r.e.v. at this scale is defined by the initial volume of the cement, V_c^0, and water, V_w^0, in the mixture:

$$|V_{II}| = V_c^0 + V_w^0 = V_c^0 \times \left(1 + \frac{\rho_c^0}{\rho_w^0} \times \frac{w}{c}\right) \tag{19}$$

where $\rho_c^0 / \rho_w^0 = 3.15$ is the cement-to-water mass density ratio, and *w/c* is the water-to-cement ratio.

In turn, the total Lagrangian porosity (Equation (4)) at early ages reads:

$$\phi \approx (1 + E_v) - \frac{\left(\Sigma_X V_X(t) + V_{C-S-H}(t) + V_{CH}(t) + V_A(t)\right)}{|V_{II}|} \tag{20}$$

where $V_X(t)$ is the volume of the four clinker phases, $V_{C-S-H}(t)$ the volume of the C-S-H matrix, $V_{CH}(t)$ the volume of the Portlandite crystals, and $V_A(t)$ the volume of the aluminates.

At this scale, the chemical porosity change is related to the dissolution of the reactants, *i.e.* $\underline{u}_X^c \cdot \underline{n}_X d\Gamma \leq 0$, and the growth of the solid hydration products (Y = C-S-H, CH, A) into the macroporosity, *i.e.* $\underline{u}_Y^c \cdot \underline{n}_Y d\Gamma \geq 0$. Expressed in terms of the volume fractions of the solid reactants and products, the change of chemical porosity reads:

$$\frac{d\phi^c}{dt} = -\left(\sum_X \frac{df_X}{dt} + \frac{df_{C-S-H}}{dt} + \frac{df_{CH}}{dt} + \frac{df_A}{dt}\right) \tag{21}$$

Fig. 4 displays the evolution of these volume fractions as a function of the overall hydration degree[2], which can be determined with hydration kinetics models of cement chemistry (see *e.g.* [33]). The key ingredient therefore for the application of the micro-chemomechanics theory turns out to be advanced hydration kinetics models. It is also readily understood from this figure that the chemical porosity is almost linearly related to the hydration degree, and the rate (Equation (21)) linearly to the hydration rate.

[2] *The overall hydration degree is defined as the weighted average of the clinker hydration degrees ξ_X [34, 35]:*

$$\xi(t) = \frac{\Sigma_X m_X \xi_X(t)}{\Sigma_X m_X}$$

where $m_X = m_{C_3S}, m_{C_2S}, m_{C_3A}, m_{C_4AF}$ are the mass fractions of the clinker phases in the cement, which are generally provided by the cement producer, based on a chemical analysis of the cement.

In other words, the chemical porosity and the overall hydration degree can be considered as equivalent macroscopic state variables. This correlation provides an interface with macroscopic thermo-chemo-mechanical models of early-age concrete that have been developed in the last decade.

3.2 Calcium leaching

Calcium, which is the dominant chemical element of cement-based materials, is leached from the material by a coupled diffusion-dissolution problem [36, 37] when concrete is in contact with water having a lower calcium concentration than some chemical equilibrium concentrations at which the probability that calcium ions in solution precipitate onto the skeleton is equal to the probability that calcium bound in the solid phase goes into solution. This process which involves tens of chemical species at very fine scales, manifests itself, at a macro-scale, by a loss of mechanical performance of concrete. Calcium leaching, which is the reference scenario for the design of nuclear waste storage systems, is a very slow process. It takes some 100 years to degrade 1m of concrete. However, this is the time-scale during which the safety of storage structures for medium- and high level nuclear waste must be ensured. The question is how?

Table 1 - Elastic moduli of the C-S-H obtained by nanoindentation w/c = 0.5

Phase	C-S-H$_a$	C-S-H$_b$
E_0 [GPa] (intact)	21.7±2.2	29.4±2.4
E_∞ [GPa] (leached)	3.0±0.8	12.0±1.2
Residual value [%]	14	41
Volume fractions	0.7	0.3

It is instructive to trace the effects of calcium leaching through the four-level microstructure of cementitious materials displayed in Fig. 1.

3.2.1 *Level I - Chemical damage of the C-S-H matrix*

Fig. 2 displays the results of nanoindentation results on a non-degraded and a calcium leached C-S-H matrix, representing asymptotic (equilibrium) states of the cement-based material. The appearance of the C-S-H matrix can be grasped from the SEM images displayed in Fig. 5, which also displays the effective material surface area of nanoindentation. The figures show that the highly disordered non-degraded C-S-H matrix becomes, after degradation, much more continuous, which is related to the dissolution and re-precipitation of C-S-H at a lower C/S-ratio [36, 38].

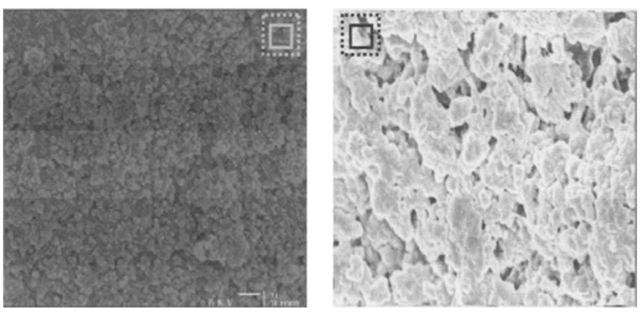

Fig. 5 - SEM images of C-S-H matrix (w/c = 0.5): Non-degraded (Top), calcium leached (Bottom). The boxes in these figures represent the effective influence zone affected by nanoindentation of a size of roughly 9 x h, where h is the penetration depth [30].

Nanoindentation at this scale provides a means of assessing the effect of calcium leaching on the material properties and volume fractions of the involved chemomechanical phases [30]. In fact, at level I the volume fraction of the two C-S-H phases is equivalent to the probability of indenting on one or the other phase. This is displayed in the histograms of Fig. 2. Remarkably, during calcium leaching (and in contrast to early-age concrete), the volume fraction of the two types of C-S-H phases does not change, despite the partial dissolution and re-precipitation process. However, that what changes during calcium leaching is the intrinsic elasticity of the C-S-H phases: The low-density C-S-H$_a$- phase has a residual stiffness of roughly 14% of its initial value, while the high-density C-S-H$_b$- phase has 41% residual stiffness (Table 1). This difference in chemical damage of the two types of C-S-H is readily understood from the morphology of the phases at level I.

The high density C-S-H$_b$- phase (inner products) degrade much less than the low-density C-S-H$_a$-phase (outer products) coating it. This finding, which sets out a new basis for the development of sustainable cement-based materials[3], provides strong evidence that the scale accessible by nanoindentation is the scale where physical chemistry meets mechanics.

3.2.2 *Level II - Micro-chemomechanics of calcium leaching*

The first phase to be dissolved, in course of calcium leaching, is the Portlandite phase that manifests itself as large crystals in the material system. The space previously occupied, at level II, by Portlandite crystals is added to the macroporosity; that is:

$$\frac{d\phi^{v}}{dt} = \frac{1}{|V_{II}|}\int_{\Gamma} \underline{u}^{CH}\cdot \underline{n}_s \, d\Gamma \ge 0 \tag{22}$$

where $\underline{u}^{CH}\cdot\underline{n}_s \le 0$ is the CH-dissolution rate at the boundary of the solid phase. Application of the micro-chemomechanics theory is straightforward [21]: The mechanical dissipation is given by Equation (14), and the chemical dissipation rate by Equation (16), reading here:

$$\varphi^{c} = \frac{1}{|V_{II}|}\int_{\Gamma}\left(\left(\frac{\rho}{\mathcal{M}}\right)_{CH}\Delta G_{CH} - \left(\psi_s^{el}+p\right)\right)\underline{u}^{CH}\cdot\underline{n}_s \, d\Gamma \ge 0 \tag{23}$$

where $\Delta G_{CH} = \mu_{Ca^{2+}} - \mu_{CH}$ is the pure chemical driving force of the dissolution, while $\psi_s^{el} + p \ge 0$ are driving forces as well, which actually accelerate the dissolution rate. It is useful to evaluate the order of magnitude of the different quantities in Equation (23), and more precisely how the strain energy compares to the pure chemical affinity ΔG_{CH}. A rough estimate of ΔG_{CH} of Portlandite dissolution, that is:

$$Ca(OH)_2 \rightarrow Ca^{2+} + 2OH^{-} \tag{24}$$

[3] *It suffices, indeed, to fine tune the mix design (particularly the w/c ratio), to increase the volume fractions of the C-S-H$_b$- phase, to obtain cement-based materials with low chemomechanical leaching tendency [26].*

is provided by considering the change in the ionic activity product $IAP = \left[\mathrm{Ca}^{2+}\right]\left[\mathrm{OH}^{-}\right]^{2}$ of the solution with regard to the solubility product K_{so} of the Portlandite, according to:

$$\max \Delta G_{CH} = \mathcal{R}\theta \ln\left(\frac{IAP}{K_{so}}\right) \tag{25}$$

where $\mathcal{R}$ = 8.314510 $\mathrm{Jmol^{-1}K^{-1}}$ is the universal gas constant and θ = 293.15 K is a reference temperature. In unleached cementitious systems, ΔG_{CH} = 0, such that $K_{so} = IAP_{eq} = \left[\mathrm{Ca}^{2+}\right]_{eq}\left[\mathrm{OH}^{-}\right]_{eq}^{2}$. A rough estimate of ΔG_{CH} can be obtained from Equation (25) by considering the change in $[\mathrm{OH}^-]$ and $[\mathrm{Ca}^{2+}]$ between the equilibrium states before and after Portlandite dissolutions. Calculations by Adenot [36] provide numerical values for the changes in concentrations of the different species in the fluid phase. The $[\mathrm{OH}^-]$concentration changes from 5 x 10^{-2} mol/l to 6 x 10^{-3} mol/l, which corresponds to pH values of 12.7 and 11.8, respectively; while the $[\mathrm{Ca}^{2+}]$concentration changes from 2.2 x 10^{-2} mol/l to 3 x 10^{-3} mol/l. Evaluating Equation (25) we find:

$$\max \Delta G_{CH} \approx -15\,\mathrm{kJmol}^{-1} \tag{26}$$

or in mechanical units

$$\left(\frac{\rho}{\mathcal{M}}\right)_{CH} \max \Delta G_{CH} \approx -450\,\mathrm{MPa} \tag{27}$$

where the Portlandite density was taken as ρ_{CH} = 2,240 kg/m^3 and the molar mass as $\mathcal{M}_{CH}$ =74.1 g mol^{-1}. The magnitude of the pure chemical driving force ΔG_{CH} needs to be compared to the elastic energy ψ_s^{el} and pressure p. Given small deformations, the elastic free energy ψ_s^{el} is smaller than 1 MPa, and the maximum fluid pressure level in the interstitial pore solution never exceeds 10 MPa. It therefore appears that both strain energy and pressure are at least one order of magnitude smaller than the pure chemical driving force, and that their effect on the chemical affinity can be neglected. This allows us to develop the chemical dissipation (Equation (23)) in the form:

$$\mathcal{A} \times \frac{d\phi^{c}}{dt} \geq 0; \mathcal{A} = \left(\frac{\rho}{\mathcal{M}}\right)_{CH} \Delta G_{CH} \tag{28}$$

Following standard thermodynamics, the dissolution kinetics is described by a law that links the 'mechanical' macro-affinity A to the change of porosity. For calcium leaching, it has been recognized that the dissolution occurs much faster compared to the diffusion process of calcium through the porosity, so that the dissolution can be considered as instantaneous. Such an instantaneous dissolution process is captured by the following dissolution law:

$$\mathcal{A} \leq 0; \frac{d\phi^{c}}{dt} \geq 0; \mathcal{A} \times \frac{d\phi^{c}}{dt} = 0 \tag{29}$$

Implemented in numerical simulation tools (finite elements or finite volumes), such an instantaneous dissolution law leads to sharp dissolution fronts [37, 39].

3.2.3 Level III - Chemical softening of friction and interface properties of mortar

The effect of calcium leaching on the mechanical behavior of mortar (level III) is quite different. The material, at this scale, is not a porous material in the sense of the poromechanics theory, but rather composed of a continuous cement paste matrix and (almost) rigid inclusions that have a common interface: the Interfacial Transition Zone (ITZ).

Fig. 6 displays SEM-images of the ITZ in the vicinity of a sand grain in a leached mortar; prior to load application (Top), and after high confinement loading (Bottom). It is readily understood from these figures that the main effect of calcium leaching on the mechanical behavior relates to the role of inclusions and of the interface properties. While many researchers have addressed by means of linear homogenization models the effect of inclusions and the ITZ properties on the elastic stiffness of mortars and concrete [40, 41], the study of the strength properties of cementitious materials by means of nonlinear continuum micromechanics is more recent [42, 43]. The underlying idea of nonlinear micromechanics is to represent the real nonlinear behavior of the composite phases and the composite by secant stress-strain relations, to homogenize the secant moduli, and analyze the homogenization result for infinite strains that define the strength limit case. We owe this 'secant method' to Suquet [44], and further developments of the method by Dormieux *et al.* [45]. Applied to mortar (level III) and concrete (level IV), or more generally to pressure sensitive materials, we distinguish:

- At high confinement, Fig. 6 (Bottom) shows that the ITZ vanishes during load application. The composite material, in its limit state, is represented as a two phase material system of a deformable matrix and rigid inclusions. For this two-phase system, application of the secant method delivers estimates of the frictional enhancement of highly filled cementitious materials [42][4]:

$$\frac{\delta_{\mathrm{hom}}}{\delta_m} = \sqrt{1 + \frac{3}{2} f_s} \tag{30}$$

where $f_s = V_s / |V_{III}|$ is the inclusion (sand) volume fraction; δ_{hom} is the composite friction coefficient, and δ_m the friction coefficient of the (cement paste) matrix. Relation (30) predicts an increase of the friction coefficient of the matrix due to the presence of rigid inclusions. This is readily understood from Fig. 6 (Bottom): the presence of rigid inclusions lead to a local confinement of the deformable matrix that is much higher than the macroscopic

[4] *In a very recent remarkable contribution, Barthélémy et al. [46] provided a refined analysis of the effect of inclusions on the friction coefficient of composite materials, based on the consistency of the local strains with the flow rule of a Drucker-Prager material, which leads to the following expression of the frictional enhancement:*

$$\frac{\delta_{\mathrm{hom}}}{\delta_m} = \sqrt{\frac{1 + \frac{3}{2} f_s}{1 - \frac{2}{3} f_s \delta_m^2}}$$

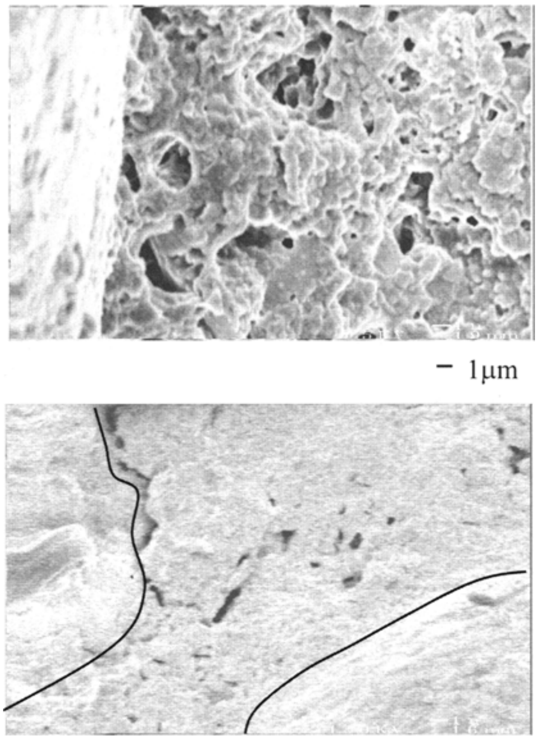

Fig. 6 - The Interfacial Transition Zone in leached mortars: Top - before load application; Bottom – after high pressure confinement [38].

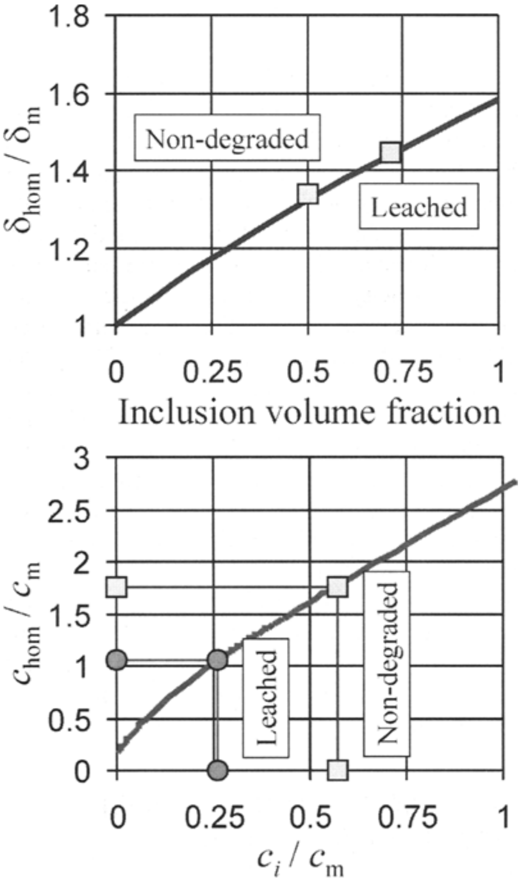

Fig. 7 - Results from nonlinear continuum micromechanics: Top - The effect of inclusions on the friction coefficient of highly filled composite materials [42]; Bottom - The effect of interfacial properties on the cohesion of highly filled composite materials [43].

confinement applied to the composite. Fig. 7 (Top) displays the predictive capability of Equation (30) for unleached and leached mortar. The experimental values of the friction coefficients of mortar and cement paste were determined from triaxial compressive tests [38, 47-49].

▪ At low confinement, the cohesion properties of mortars and concrete are governed by the interfacial properties. Application of the secant method to a three phase representation of the composite materials, delivers the cohesion of the composite as a function of the volume fractions of the inclusions, f_s, and the ITZ, f_i, and the interface-to-matrix cohesion ratio $\chi = c_i/c_m$; that is [43, 38]:

$$\frac{c_{\mathrm{hom}}}{c_m} = \mathcal{F}(f_s, f_i, c_i / c_m) \tag{31}$$

While relation (31) does not permit an analytical representation, the inverse application of the model allows one to assess the chemical softening of the interfacial properties of mortar and concrete. This is displayed in Fig. 7 (Bottom). The input parameters are the volume fractions of the inclusions and of the interface (the first is known from the mix design, here $f_s = 0.5$, the second from the SEM-investigation, here $f_i = 0.3$), and the mortar-to-cement paste cohesion ratio that can be determined from uniaxial compression and uniaxial tension test results (here $(c_{\mathrm{hom}}/c_m)^0 = 1.76$ for the non-degraded materials, and $(c_{\mathrm{hom}}/c_m)^\infty = 1.05$ for the asymptotically leached materials). Use of these values in relation (31) provides an assessment of the interface-to-matrix cohesion ratio $\chi = c_i/c_m$ for the two-asymptotic states:

$$\chi^0 = 0.57; \; \chi^\infty = 0.26 \tag{32}$$

The values highlight the strong chemical softening of the ITZ-cohesion, which is much higher than the chemical softening of the matrix. This is readily understood from the chemical composition of the ITZ, which is known to be a zone of higher Portlandite concentration. This leads, after leaching, to a material that is much more sensitive, at failure, to the ITZ properties.

In summary, nonlinear continuum micromechanics provides a rational means of determining the asymptotic states of the chemical softening of the strength parameters undergone by mortar (level III) and concrete (level IV) in the course of calcium leaching.

3.2.4 Summary: multiscale chemomechanics of calcium leaching of concrete

The underlying idea of the chemomechanics approach for calcium leaching presented here is to (1) experimentally and theoretically assess at multiple scales the two asymptotic states of aging of cement-based materials, *i.e.* the initial intact non-degraded material and final homogeneously leached material states, and (2) to bridge these asymptotic states by means of a multiscale constitutive modeling of the chemomechanical deterioration kinetics. We borrow this approach from physical chemistry, in which thermodynamic equilibrium states are assessed, but employ it here for chemomechanical properties and deformation behavior of the solid.

The multiscale representation of cementitious materials suggests the following three chemomechanical equilibrium

Table 2 - Summary of the values for the poroelastic properties for a w/c-0.5 cementitious material [51]: K = drained bulk modulus, G = shear modulus, b = Biot coefficient, N = Skeleton Biot modulus, K_u = undrained bulk modulus, M = overall Biot modulus, B = Skempton coefficient; f_s = sand volume fraction

Properties	Intact	CH leached	C-S-H leached
Level I: C-S-H matrix (w/c = 0.5)			
K^{I}_{hom} [GPa]	15.2	15.2	2.7
G^{I}_{hom} [GPa]	9.6	9.6	1.7
Level II: Cement paste (w/c = 0.5)			
K^{II}_{hom} [GPa]	15.4	11.2	1.7
G^{II}_{hom} [GPa]	9.4	7.3	1.1
b^{II} [1]	0.07	0.26	0.37
N^{II} [GPa]	1170	124	17
$K^{u,II}_{\text{hom}}$ [GPa]	15.7	12.2	2.6
M^{II} [GPa]	72	15	6.7
B^{II} [1]	0.30	0.31	0.94
Level III: Mortar (w/c = 0.5;f_s = 0.5)			
K^{III}_{hom} [GPa]	22.9	19.4	4.5
G^{III}_{hom} [GPa]	15.2	15.3	3.1
b^{III} [1]	0.04	0.18	0.34
N^{III} [GPa]	2339	248	35
$K^{u,III}_{\text{hom}}$ [GPa]	23.2	20.3	6.0
M^{III} [GPa]	144	29	13.5
B^{III} [1]	0.26	0.25	0.76

Table 3 – Summary of the values for the strength properties. The asymptotic values for levels II and III were determined experimentally, while the intermediate states (CH leached) and the level I values were determined with nonlinear continuum micromechanics [38]: δ = friction coefficient; c = cohesion

Properties	Intact	CH leached	leached
High confinement			
Level I: C-S-H matrix (w/c=0.5)			
δ [1]	0.85	0.85	0.71
c [GPa]	18.01	18.01	1.26
Level II: Cement paste (w/c=0.5)			
δ [1]	0.82	0.71	0.56
c [GPa]	17.11	14.5	1.15
Level III: Mortar (w/c = 0.5;f_s = 0.5)			
δ [1]	1.02	0.94	0.81
c [GPa]	9.82	9.13	0.96
Low confinement			
Level I: C-S-H matrix (w/c=0.5)			
δ [1]	1.67	1.67	1.26
c [GPa]	2.2	2.2	1.05
Level II: Cement paste (w/c=0.5)			
δ [1]	1.62	1.39	0.99
c [GPa]	2.09	1.8	0.79
Level III: Mortar (w/c = 0.5;f_s = 0.5)			
δ [1]	1.43	1.34	0.91
c [GPa]	3.67	3.41	0.83

states: the intact material, an intermediate state defined by the dissolution of Portlandite at level II, and finally the asymptotically leached material defined by the decalcification of the C-S-H matrix at level I. Table 2 summarizes the poroelastic properties of these three material states for a w/c = 0.5 cementitious material. The input parameters are only nanoindentation results and volume fractions of the involved phases. Similarly, Table 3 summarizes the strength parameters of the material. Combined with chemoporoplasticity models that allow modeling the simultaneous chemical damage, chemical softening and plastic softening [9, 18, 19, 38], prediction, anticipation and mitigation of the deterioration of the load bearing capacity of materials and structures subjected to calcium leaching becomes possible.

By way of application, Figs. 8 and 9 display results from model-based simulations of residual 4-point bending strength tests presented by Schneider and Chen [52]. The tests were performed on mortar beams produced at a water-cement ratio of w/c = 0.5 from a Type I Portland cement and a fine sand. The beams have a size of 40 mm x 40 mm x 160 mm, and were subjected to accelerated calcium leaching. At different times between 7 days and 821 days, specimens were taken from the bath and tested in four-point bending.

The results are reported by Schneider and Chen as a plot of the ratio β/β_{28} versus time. β is the maximum equivalent tensile stress in the beam calculated under the assumption of a linear stress distribution over the beam section:

$$\beta = \frac{6M}{bh^2} \tag{33}$$

where M is the bending moment, b and h are the width and height of the beam section, respectively. The index 28 refers to the strength measured on intact specimens after 28 days of curing. The β_{28} value is 8.3 MPa, corresponding to a bending moment of M_{28} = 88.5 Nm. Fig. 8 displays the results of the two-front dissolution-diffusion simulation for different leaching times; and Fig. 9 displays the normalized bending moment capacity as a function of the leaching time, for two molar concentrations of the ammonium nitrate solution: 0.85M and 6M. Schneider and Chen [52] reported to have used a 10% ammonium nitrate solution, corresponding to a concentration of 68 g NH_4NO_3 per kilogram of solution, that is a 0.85M ammonium nitrate solution. However, the model-based chemomechanics simulation results indicate that the one which matches best the overall load-bearing capacity in time is leaching in a 6M ammonium nitrate solution.

Given the almost perfect correlation of experimental versus model-based simulation results of the bending strength decay, it is likely that the actual leaching conditions of Schneider and Chen's test may well correspond to a 6M solution.

4. CONCLUDING REMARKS: FROM CHEMOMECHANICS TO BIO-CHEMOMECHANICS

Concrete, like many other materials (whether man-made, geological or biological) are highly heterogeneous materials, with heterogeneities that manifest themselves at multiple

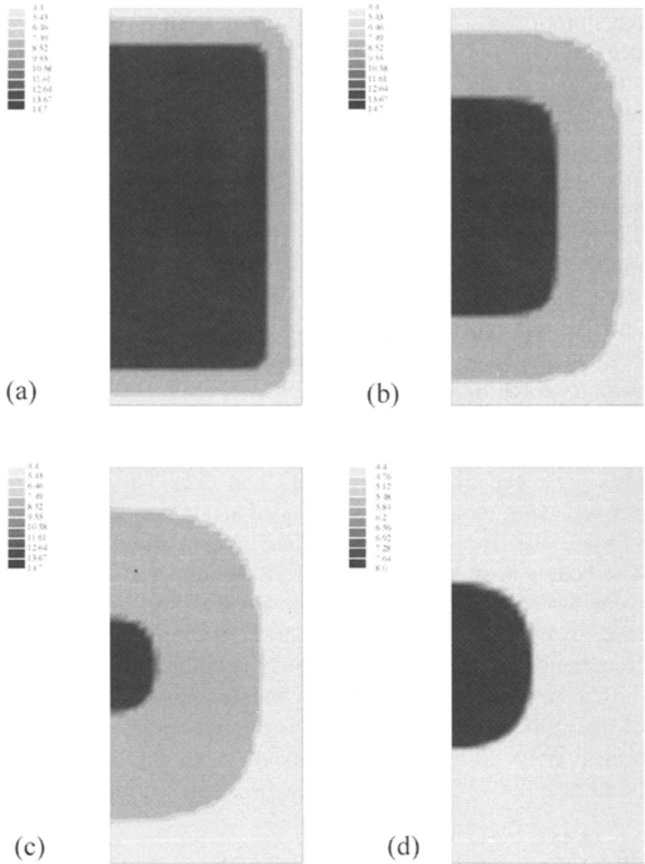

Fig. 8 - Results from the leaching calculation with the 6M ammonium nitrate solution. (a) 7 days, (b) 35 days, (c) 84 days and (d) 182 days of leaching. The result values are solid calcium concentrations in mol/l in the mid-span beam section [Results with CESAR-LCPC@MIT]; [38].

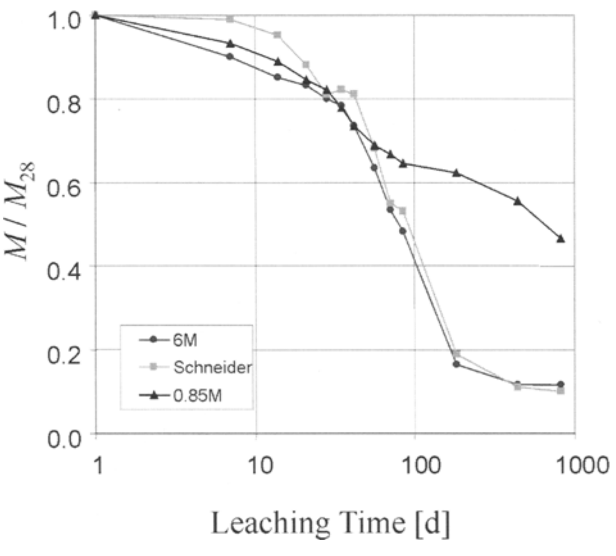

Fig. 9 - Model based simulations of the change in bending strength with two different leaching boundary conditions in comparison with the experimental data by Schneider and Chen [52]; [simulation results with CESAR-LCPC@MIT].

scales. As new experimental techniques such as nanoindentation have provided unprecedented access to micro-mechanical properties of materials, it becomes possible to identify the mechanical effects of chemical reactions at the micro-scale, where the reactions occur, and trace these micro-chemomechanical effects through upscaling techniques to the macro-scale. The identification of the length scales where physical chemistry meets (solid) mechanics appears to us as a key to prediction and anticipation of material deterioration. This approach is not restricted to geomaterials, but equally applies to biological materials, and biodegradation processes in which cell-mediated biological processes interact with solid matter affecting the mechanical performance of the solid.

While the link between biological processes and chemical effects has been a focus of biochemistry, the integration of biological processes into a consistent framework of chemomechanics is challenging. The main difficulty arises from the very nature of biological processes: Biological processes are dynamic in nature, and not defined with respect to an equilibrium state, in contrast to both mechanical processes and chemical processes. In addition, the absence of biological conservation laws complicates the direct integration of biological processes into the constitutive modeling of the material behavior.

On the other hand, the consideration of the solid material system as thermodynamic system provides a means of addressing this problem. In this case, the solid witnesses the biological activity through the biochemical conditions generated at the solid surface where cells or microorganisms attach. This is, in a nutshell, the way by which micro-chemomechanics can be extended to bio-chemomechanics [53], and leads to a similar split of the overall behavior of the porous materials as in chemomechanics: the purely mechanical response is captured by the poromechanics theory (*i.e.* Equation (15)), and the bio-chemomechanical response by the moving boundary problem; that is analogously to relation (16):

$$\varphi^{c} = -\mathcal{A} \circ \frac{d\phi^{c}}{dt} = \frac{1}{|V|} \int_{\Gamma} A \times J_{N} d\Gamma \geq 0 \qquad (34)$$

with

$$A = \mu^{BGP} - \mu_{c} - \left(\frac{\mathcal{M}}{\rho_{c}}\right)\left(\psi_{s}^{el} + p\right) \qquad (35)$$

where μ^{BGP} is the biological generated potential on surface $\Gamma \subseteq \partial V_{s}$ where biological organisms attach. The pure biochemical driving force $\Delta G = \mu^{BGP} - \mu_{c}$ is given by biochemistry, while the additional terms $\psi_{s}^{el} + p$ relate to the solid deformation and the liquid pressure prevailing in the porosity.

The porosity generated by the biochemical activity follows from Equation (6), and can be developed in the form:

$$\frac{d\phi^{bc}}{dt} = \frac{\mathcal{N}}{\mathcal{L}_{p}} \times \frac{1}{\Gamma} \int_{\Gamma} -\underline{u}^{bc} \cdot \underline{n}_{s} d\Gamma \qquad (36)$$

where $\mathcal{L}_{p} = |V| / |\partial V_{s}|$ is the total volume to solid surface ratio of the porous material; $\mathcal{N} = \Gamma / |\partial V_{s}|$ is the solid surface fraction occupied by cells or microorganisms, while the quantity $\frac{1}{\Gamma} \int_{\Gamma} -\underline{u}^{bc} \cdot \underline{n}_{s} d\Gamma$ represents the average biologically induced solid resorption or deposition activity of cells or microorganisms. While the first parameter $\mathcal{L}_p$ relates to the morphology of the porous material, the second parameter $\mathcal{N}$ relates to the biological population density, and provides the link with biological population models. Finally, the third quantity relates to the average biochemical activity, eventually amplified by the strain energy in the solid and the interstitial pore pressure (see Equation (35)). While the average strain energy is generally some orders of magnitude smaller than the biological generated potential, the strain energy in the immediate surrounding of cracks increases due to stress concentrations to a value that often compares to the one of the biologically generated potential. This phenomenon has been suggested as one possible origin of the self-healing adaptive capacity of living tissues as bones [53], which are remodeled continuously during adulthood through the resorption of old bone by Osteoclasts and the subsequent formation of new bone by Osteoblasts (see Fig. 10): In the course of random remodelling events by cells, the chemomechanical coupling is a nonrandom remodelling stimulus, initiating the repair of damage in bone, which at the same time reduces by resorption the risk of crack propagation. What a great potential as construction material?

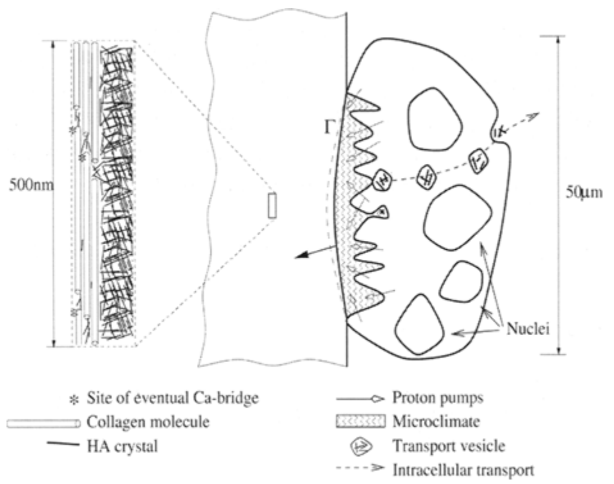

Fig. 10 - Biologically mediated chemomechanical dissolution process: osteoclast resorption on a bone surface [53].

ACKNOWLEDGMENT

Financial support for chemomechanics research at MIT was provided by the Nuclear Energy Research Initiative of the US-Department of Energy, the Esther & Harold E. Edgerton Chair at M.I.T., the Lafarge Corporation (France), and through the postdoctoral fellowships by the Kade Foundation, New York, administered through the Austrian Academy of Sciences, for Dr. Christian Hellmich, and by the Swiss Science Foundation for Dr. Olivier Bernard. The nanoindentation tests were performed in Prof. Subra Suresh's NanoLab at M.I.T. under the supervision of Dr. Krystyn Van Vliet, whose assistance is gratefully acknowledged. Last, a special thanks to the CESAR-LCPC development team at Laboratoire Central des Ponts et Chaussées, Paris, for maintenance of CESAR-LCPC@MIT.

REFERENCES

[1] Coussy, O., 'Mechanics of porous media', (J. Wiley & Sons, Chichester, UK, 1995).

[2] Coussy, O. and Ulm, F.-J., 'Creep and plasticity due to chemo-mechanical couplings', *Archive of Applied Mechanics* **66** (1996) 523-535.

[3] Sercombe, J., Ulm, F.-J. and Mang, H.A., 'Consistent return mapping algorithm for chemoplastic constitutive laws with internal couplings', *Int. J. Numerical Methods in Engineering* **47** (2000) 75-100.

[4] Ulm, F.-J. and Coussy, O., 'Modeling of thermo-chemomechanical couplings of concrete at early ages', *Journal of Engineering Mechanics, ASCE* **121** (7) (1995) 785-794.

[5] Ulm, F.-J. and Coussy, O., 'Couplings in early-age concrete: from material modeling to structural design', *Int. Journal of Solids and Structures* **35** (31-32) (1998) 4295-4311.

[6] Cervera, M., Oliver, J. and Prato, T., 'Thermo-chemo-mechanical model for concrete. I: Hydration and aging', *Journal of Engineering Mechanics, ASCE* **125** (9) (1999) 1018-1027.

[7] Cervera, M., Oliver, J. and Prato, T., 'Thermo-chemo-mechanical model for concrete. II: Damage and creep, *Journal of Engineering Mechanics, ASCE* **125** (9) (1999) 1028-1039.

[8] Sercombe, J., Hellmich, C., Ulm, F.-J. and Mang, H.A., 'Modeling of early-age creep of shotcrete. I: Model and model parameters', *Journal of Engineering Mechanics, ASCE* **126** (3) (2000) 284-291.

[9] Ulm, F.-J. and Coussy, O., 'Strength growth as chemo-plastic hardening in early age concrete', *Journal of Engineering Mechanics, ASCE* **122** (12) (1996) 1123-1132.

[10] Hellmich, C., Ulm, F.-J. and Mang, H.A., 'Multisurface chemoplasticity. I: Material model for shotcrete', *Journal of Engineering Mechanics, ASCE* **125** (6) (1999) 692-701.

[11] Hellmich, C., Ulm, F.-J. and Mang, H.A., 'Consistent linearization in finite element analysis of coupled chemo-thermal problems with exo- or endothermal reactions', *Computational Mechanics* **24** (4) (1999) 238-244.

[12] Ulm, F.-J. and Coussy, O., 'What is a 'massive' concrete structure at early ages? - Some dimensional arguments', *Journal of Engineering Mechanics, ASCE* **127** (5) (2001) 512-522.

[13] Ulm, F.-J., Coussy, O. and Bažant, Z.P., 'The 'Chunnel' fire. I. Chemoplastic softening in rapidly heated concrete', *Journal of Engineering Mechanics, ASCE* **125** (3) (1999) 272-282.

[14] Larive, C., 'A combined experimental-theoretical approach for the understanding of the alkali reaction and of its mechanical effects', Monograph LPC OA 28, (Laboratoires des Ponts et Chaussées, Paris) [in French, partially translated into English](1998).

[15] Ulm, F.-J., Coussy, O., Li, K. and Larive, C., 'Thermo-chemo-mechanics of ASR-expansion in concrete structures', *Journal of Engineering Mechanics, ASCE* **126** (3) (2000) 233-242.

[16] Li, K. and Coussy, O., 'Concrete ASR degradation: from material modeling to structure assessment', *Concrete Science and Engineering*, RILEM **4** (13) (2002) 35-46.

[17] Li, K., 'Chemomechanics modeling of the behavior of concrete affected by the alkali-silica reaction and model-based assessment of degraded structures', PhD Dissertation, Ecole Nationale des Ponts et Chaussées, Paris, France [in French](2002).

[18] Ulm, F.-J., Peterson, M. and Lemarchand, E., 'Is ASR-Expansion caused by chemoporoplastic dilatation?', *Concrete Science and Engineering* **4** (13) (2002) 47-55.

[19] Ulm, F.-J., Torrenti, J.M. and Adenot, F., 'Chemoporoplasticity of calcium leaching in concrete', *Journal of Engineering Mechanics, ASCE* **125** (10) (1999) 1200-1211.

[20] Ulm, F.-J. and Coussy, O., 'Mechanics and Durability of Solids. Vol. I - Solid Mechanics', (MIT-Prentice Hall Textbook Series in Civil, Environmental and Systems Engineering, Upper Saddle River, NJ, 2002).

[21] Ulm, F.-J., Lemarchand, E. and Heukamp, F.H., 'Elements of chemomechanics of Calcium leaching of cement-based materials at different scales', *Journal of Engineering Fracture Mechanics* **70** (2003) 871-889.

[22] Constantinides, G. and Ulm F.-J., 'The elastic properties of calcium-leached cement pastes and mortars: a multi-scale investigation', MIT-CEE Report R02-01, (MSc Dissertation, M.I.T.), Cambridge, MA, 2002.

[23] Tennis, P.D. and Jennings, H.M., 'A model for two types of calcium silicate hydrate in the microstructure of Portland cement paste', *Cement and Concrete Research* **30** (6) (2000) 855-863.

[24] Jennings, H.M., 'A model for the microstructure of calcium silicate hydrate in cement paste', *Cement and Concrete Research* **30** (1) (2000) 101-116.

[25] Acker, P., 'Micromechanical analysis of creep and shrinkage mechanisms', in F.-J. Ulm, Z.P. Bažant and F.H. Wittmann (Eds.), 'Creep, shrinkage and durability mechanics of concrete and other quasi-brittle materials', Proc. of the Sixth International Conference CONCREEP-6@MIT, Elsevier, Oxford (UK), 2001 15-25.

[26] Constantinides, G. and Ulm, F.-J., 'The effect of two types of C-S-H on the elasticity of cement-based materials: results from nanoindentation and micromechanical modeling', *Cement and Concrete Research* (in press).

[27] Bažant, Z.P., 'Thermodynamics of interacting continua with surfaces and creep analysis of concrete structures', *Nuclear Engineering and Design* **20** (1972) 477-505.

[28] Wittmann, F.H., 'Creep and shrinkage mechanisms', in Z.P. Bažant & F.H. Wittmann (Eds.), 'Creep and shrinkage of concrete structures', (J. Wiley and Sons, 1982) 129-161.

[29] Velez, K., Maximilien, S., Damidot, D., Fantozzi, G. and Sorrentino, F., 'Determination by nanoindentation of elastic modulus and hardness of pure constituents of Portland cement clinker', *Cement and Concrete Research* **31** (4) (2001) 555-561.

[30] Constantinides, G., Ulm, F.-J., Van Vliet, K.J., 'On the use of nanoindentation for cementitious materials', *Mater. Struct. (Special issue of Concrete Science and Engineering)* **36** (257) (2003) 191-197.

[31] Zaoui, A., 'Continuum micromechanics - A survey', *Journal of Engineering Mechanics, ASCE* **128** (8) (2002) 808-816.

[32] Mori, T. and Tanaka, K., 'Average stress in matrix and average elastic energy of materials with misfitting inclusions', *Acta Metallurgica* **21** (5) (1973) 1605-1609.

[33] Bernard, O., Ulm, F.-J. and Lemarchand, E., 'A multiscale micromechanics-hydration model for the early-age elastic properties of cement-based materials', *Cement and Concrete Research* (2003) (in press).

[34] Powers, T.C. and Brownyard, T.L., 'Studies of the physical properties of hardened Portland cement paste', *Journal of the American Concrete Institute* **18** (1946) 101-132.

[35] Taylor, H.F.W., 'Cement Chemistry', (Academic Press, New York, 1997).

[36] Adenot, F., 'Durabilité du béton : caractérisation et modélisation des processus physique et chimiques de dégradation du ciment', PhD Dissertation, Université d'Orléans, France, 1992.

[37] Mainguy, M. and Coussy, O., 'Propagation fronts during calcium leaching and chloride penetration', *Journal of Engineering Mechanics, ASCE* **126** (3) (2000) 250-257.

[38] Heukamp, F.H. and Ulm, F.-J., 'Chemomechanics of calcium leaching of cement-based materials at different scales: The role of CH-dissolution and C-S-H degradation on strength and durability performance of materials and structures", MIT-CEE Report R02-03 (PhD Dissertation, M.I.T.), Cambridge, MA, 2002.

[39] Mainguy, M., Ulm, F.-J. and Heukamp, F.H., 'Similarity properties of demineralization and degradation of cracked porous materials', *Int. Journal of Solids and Structures* **38** (2001) 7079-7100.

[40] Garboczi, E.J., 'Computational materials science of cement-based materials', *Mater. Struct.* **26** (2) (1993) 191-195.

[41] Li, G.Q., Zhao, Y., Pang, S.S. and Li, Y.Q., 'Effective Young's modulus estimation of concrete', *Cement and Concrete Research* **29** (9) (1999) 1455-1462.

[42] Lemarchand, E., Ulm, F.-J. and Dormieux, L., 'Effect of inclusions on friction coefficient of highly filled composite materials', *Journal of Engineering Mechanics, ASCE* **128** (2002) (8) 876-884.

[43] Heukamp, F.H, Lemarchand, E. and Ulm, F.-J., 'The effect of interfacial properties on the cohesion of highly filled composites', *Int. Journal of Solids and Structures* (in press).

[44] Suquet, P., 'Effectives properties of nonlinear composites", In: P. Suquet (Ed.), Continuum micromechanics, CISM 377, Springer-Verlag, Wien, 1997.

[45] Dormieux, L., Molinari, A. and Kondo, D., 'Micromechanical approach to the behavior of poroelastic materials', *J. Mech. Phys. Solids* **29** (2002) (8) 2203-2231.

[46] Barthélémy, J.F., Dormieux, L. and Lemarchand, E., 'A micromechanical approach to the strength criterion of composite materials', in N. Bicanic, R. de Borst, H. Mang and G. Meschke, Proc. Euro-C 2003, Computational Modelling of Concrete Structures, St. Johann im Pongau, Austria, March 2003, A.A. Balkema, Lisse, The Netherlands, 53-58, 2003.

[47] Heukamp, F.H., Ulm, F.-J. and Germaine, J.T., 'Mechanical properties of calcium leached cement pastes: Triaxial stress states and the influence of the pore pressure', *Cement and Concrete Research* **31** (5) (2001) 767-774.

[48] Ulm, F.-J., Heukamp, F.H. and Germaine, J.T., 'Residual design strength of cement-based materials for nuclear waste storage systems', Nuclear Engineering and Design 211(1) (2002) 51-60.

[49] Heukamp, F.H., Ulm, F,-J. and Germaine, J.T., 'Poroplastic properties of calcium leached cement-based materials', *Cement and Concrete Research*, In press, 2003.

[50] Ulm, F.-J., Coussy, O. and Hellmich, Ch., 'Chemoplasticity: a review of evidence', in R. de Borst, N. Bicanic, H. Mang and G. Meschke, Proc. Euro-C'98, 'Computational Modelling of Concrete Structures', Bad Gastein, Austria, March/April 1998, A.A. Balkema, Rotterdam, 1998, 421-439.

[51] Ulm, F.-J., Heukamp, F.H. and Constantinides, G., 'Is concrete a poromechanics material? - A multiscale investigation of poroelastic properties', *Mater. Struct., Special issue of Concrete Science and Engineering* (2003) (in review).

[52] Schneider, U. and Chen, S.-W., 'The chemomechanical effect and the mechanochemical effect on high-performance concrete subjected to stress corrosion', *Cement and Concrete Research* **28** (4) (1998) 509-522.

[53] Silva, E.C. and Ulm, F.-J., 'A bio-chemo-mechanics approach to bone remodeling and fracture', in B.L. Karihaloo (Ed.) Proc. IUTAM Symposium, Analytical and Computational Fracture Mechanics of Non-Homogeneous Materials, Cardiff June 2001, Kluwer Academic Publishers, Dordrecht-Boston-London (2002) 355-366.

Paper received: December 19, 2002; Paper accepted: April 5, 2003